

# Ammonia and other parent molecules in comet 10P/Tempel 2 from *Herschel*/HIFI<sup>★</sup> and ground-based radio observations

N. Biver<sup>1</sup>, J. Crovisier<sup>1</sup>, D. Bockelée-Morvan<sup>1</sup>, S. Szutowicz<sup>2</sup>, D.C. Lis<sup>3</sup>, P. Hartogh<sup>4</sup>, M. de Val-Borro<sup>4</sup>, R. Moreno<sup>1</sup>, J. Boissier<sup>5,6</sup>, M. Kidger<sup>7</sup>, M. Küppers<sup>7</sup>, G. Paubert<sup>8</sup>, N. Dello Russo<sup>9</sup>, R. Vervack<sup>9</sup>, H. Weaver<sup>9</sup>, and HssO team

<sup>1</sup> LESIA, Observatoire de Paris, CNRS, UPMC, Université Paris-Diderot, 5 place Jules Janssen, 92195 Meudon, France. e-mail: Nicolas.Biver@obspm.fr

<sup>2</sup> Space Research Centre, PAS, Warszawa, Poland

<sup>3</sup> Caltech, Pasadena, CA, USA

<sup>4</sup> Max Planck Institut für Sonnensystemforschung, Katlenburg-Lindau, Germany

<sup>5</sup> Istituto di Radioastronomia - INAF, Bologna, Italy

<sup>6</sup> ESO, Garching bei München, Germany

<sup>7</sup> ESAC, Villafranca del Castillo, Spain

<sup>8</sup> IRAM, Avd. Divina Pastora, 7, 18012 Granada, Spain

<sup>9</sup> JHU/APL, Laurel, Maryland, USA

Draft May 28, 2018

## ABSTRACT

The Jupiter-family comet 10P/Tempel 2 was observed during its 2010 return with the *Herschel Space Observatory*. We present here the observation of the  $J_K(1_0-0_0)$  transition of  $\text{NH}_3$  at 572 GHz in this comet with the Heterodyne Instrument for the Far Infrared (HIFI) of *Herschel*. We also report on radio observations of other molecules (HCN,  $\text{CH}_3\text{OH}$ ,  $\text{H}_2\text{S}$  and CS) obtained during the 1999 return of the comet with the CSO telescope and the JCMT, and during its 2010 return with the IRAM 30-m telescope. Molecular abundances relative to water are 0.09%, 1.8%, 0.4%, and 0.08% for HCN,  $\text{CH}_3\text{OH}$ ,  $\text{H}_2\text{S}$ , and CS, respectively. An abundance of 0.5% for  $\text{NH}_3$  is obtained, which is similar to the values measured in other comets. The hyperfine structure of the ammonia line is resolved for the first time in an astronomical source. Strong anisotropy in the outgassing is present in all observations from 1999 to 2010 and is modelled to derive the production rates.

**Key words.** comets: individual: 10P/Tempel 2 – radio lines – submillimetre – techniques: spectroscopic

## 1. Introduction

With an abundance of  $\approx 0.5\%$  relative to water, ammonia is a major repository of nitrogen in cometary volatiles (Bockelée-Morvan et al. 2004). The photodissociation products of  $\text{NH}_3$ ,  $\text{NH}_2$  and  $\text{NH}$ , are routinely observed in the visible spectra of comets (Feldman et al. 2004). The direct observation of ammonia is difficult because it is a short-lived molecule (lifetime  $\approx 5000$  s at 1 AU from the Sun) and because its lines are either weak or affected by telluric absorption.

In previous radio observations of  $\text{NH}_3$ , the inversion transitions near 24 GHz were tentatively detected with ground-based radio telescopes in C/1983 H1 (IRAS-Araki-Alcock) (Altenhoff et al. 1983), but not in 1P/Halley (Bird et al. 1987). They were then definitely detected in C/1996 B2 (Hyakutake) (Palmer et al. 1996) and C/1995 O1 (Hale-Bopp) (Bird et al. 1997; Hirota et al. 1999) and tentatively detected in 153P/Ikeya-Zhang (Bird et al. 2002; Hatchell et al. 2005).

Ammonia rotational lines are expected to be much stronger, but they fall in the submillimetric spectral range and have to be observed from space. The  $J_K(1_0-0_0)$  line at 572.5 GHz was first detected in C/2001 Q4 (NEAT) and C/2002 T7 (LINEAR) with the Odin satellite (Biver et al. 2007).

Ammonia was also observed from its  $\nu_1$  and/or  $\nu_3$  vibrational bands near  $3 \mu\text{m}$  in comets 6P/d'Arrest, 73P/Schwassmann-Wachmann 3, C/1995 O1 (Hale-Bopp), C/2002 T7 (LINEAR), C/2004 Q2 (Machholz), C/2006 P1 (McNaught), and 103P/Hartley 2 (Kawakita & Mumma 2011, and references therein).

Comet 10P/Tempel 2 is a Jupiter-family comet discovered in 1873 by Wilhelm Tempel. Its orbital period is 5.5 years; thus alternate perihelion passages are favourable. Its behaviour has already been well documented, 2010 being the year of the 22<sup>nd</sup> return to perihelion observed for this comet. Prior to 1994, its perihelion distance was shorter ( $\approx 1.31-1.39$  AU vs 1.48 AU), resulting in a closer approach to the Earth and the comet being more active at perihelion. After the 1999 apparition, the orbit of the comet slightly changed and the perihelion distance decreased again to 1.42 AU.

Comet 10P/Tempel 2 has a relatively large nucleus ( $\approx 16 \times 8$  km; Jewitt & Luu 1989; Lamy et al. 2009), and a well-studied rotation period of  $\approx 8.95$  h, found to be increasing with time (Knight et al. 2011). Given its relatively low outgassing rate, only a small fraction of its nucleus is active. Strong seasonal effects are observed: the activity rises very rapidly during the last three months before perihelion and peaks about one month after. A prominent dust jet close to the north pole has been observed in images at each perihelion.

<sup>★</sup> *Herschel* is an ESA space observatory with science instruments provided by European-led Principal Investigator consortia and with important participation from NASA.

We report on an observation of the 572.5 GHz line of ammonia in comet 10P/Tempel 2, which was part of the study of this comet with the *Herschel Space Observatory*. Preliminary reports were given by Biver et al. (2010) and Szutowicz et al. (2011). Additional analyses of the observations of water with the Heterodyne Instrument for the Far Infrared (HIFI) in this comet will be presented by Szutowicz et al. (2012 in preparation). Several water lines were also detected with the Photodetector Array Camera and Spectrometer (PACS) and the Spectral and Photometric Imaging Receiver (SPIRE) instruments of *Herschel* and will be presented in a future paper.

In support of *Herschel* observations, 10P/Tempel 2 was observed from the ground at millimetric wavelengths with the Institut de radioastronomie millimétrique (IRAM) 30-m telescope. We also present observations obtained at the antepenultimate perihelion passage (in 1999), with the Caltech Summillimeter Observatory (CSO) telescope and the James Clerk Maxwell Telescope (JCMT), which helped to prepare the *Herschel* observations.

## 2. Observations

The 1999 perihelion of comet 10P/Tempel 2 was on 8 September at  $r_h = 1.48$  AU. The perigee took place on 12 July at 0.65 AU. HCN was observed at JCMT on 4 and 6 September, and again on 1 and 2 October. HCN was also observed at CSO on 11 and 12 September (Fig. 3) and CH<sub>3</sub>OH on the 12th only.

The 2010 perihelion was on 4 July at  $r_h = 1.42$  AU and perigee took place on 26 August at  $\Delta = 0.65$  AU. The comet was observed with the IRAM 30-m radio-telescope between 7.2 and 11.4 July 2010 UT. The first two nights suffered from bad weather and the third was completely lost, but days 4 and 5 yielded good data (Figs. 4–6). Table 1 provides the list of detected lines.

Comet 10P was also observed in 2010 with the *Herschel Space Observatory* (Pilbratt et al. 2010) using HIFI (de Graauw et al. 2010), within the framework of the *Water and related chemistry in the Solar System* (HssO) project (Hartogh et al. 2009). Several water rotational lines were observed and mapped from 15 June to 29 July 2010 (Szutowicz et al. 2011, 2012 in preparation). The observation of ammonia took place on 19.1 July 2010 UT when the comet was at  $r_h = 1.43$  AU and at  $\Delta = 0.71$  AU from *Herschel*. The  $J_K(1_0-0_0)$  transition of NH<sub>3</sub> at 572.5 GHz and the  $1_{10-1_01}$  line of H<sub>2</sub>O at 557 GHz were observed simultaneously in the frequency-switching mode, the former in the upper side band and the latter in the lower side band of the band 1b receiver of HIFI. A total of 54 min of integration time were spent on the comet, split into five observations every 2 h to cover a full rotation of the nucleus. Water and ammonia were observed both with the low-resolution spectrometer (WBS, resolution 0.58 km s<sup>-1</sup>) and the highest resolution mode of the high-resolution spectrometer (HRS autocorrelator, resolution 0.074 km s<sup>-1</sup>) and both polarizations were averaged (Figs 1, 2).

## 3. Results

### 3.1. Modelling the data

The same excitation and outgassing pattern model has been used to analyse all data. The density distribution is based on the Haser model, with photodissociation rates at 1 AU,  $\beta_0 \approx 1.88 \times 10^{-5}$  s<sup>-1</sup> in 1999 and  $\beta_0 = 1.60 \times 10^{-5}$  s<sup>-1</sup> in 2010, for HCN, based on the solar activity. The gas temperature is constrained by the

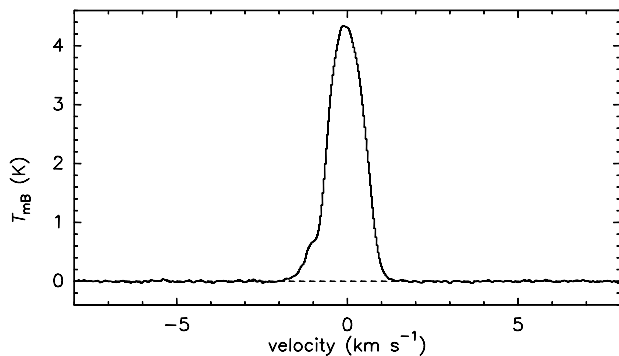


**Fig. 1.** Water H<sub>2</sub>O( $1_{10-1_01}$ ) line observed in comet 10P/Tempel 2 with *Herschel* using the HRS on 19 July 2010.

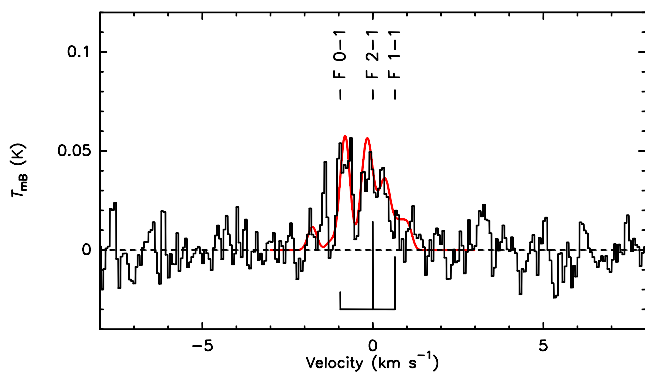


**Fig. 2.** Ammonia  $J_K(1_0-0_0)$  line observed in comet 10P/Tempel 2 with *Herschel* using the HRS on 19 July 2010. The position and relative intensities of the hyperfine components are shown with a synthetic spectrum overlotted that takes into account hyperfine structure and asymmetric outgassing (see text).

rotational temperature of methanol lines and the outgassing pattern and expansion velocity are constrained by the line shapes. Collisions with electrons are taken into account as modelled in Zakharov et al. (2007) with a density scaling factor  $x_{ne}$  of 0.5 (Biver et al. 2006).

All lines (Figs. 3–5) show a strong asymmetry (mean Doppler shift around  $-0.3$  to  $-0.4$  km s<sup>-1</sup>, Table 1) and need to be modelled with asymmetric outgassing. The strong blueshift and a phase angle ( $\approx 42^\circ$ ) smaller than  $90^\circ$  suggest that a large part of the outgassing is dominated by a relatively narrow jet on the day-side that is not far from the direction to the Earth. The opening of the jet and the fraction of outgassing it contains were constrained by the Doppler shifts of the lines and optimized to fit the line shapes. The half width at half maximum (HWHM) of the lines on the negative and positive sides suggests expansion velocities of 0.9 and 0.5 km s<sup>-1</sup> on the day and night sides, respectively.

The rotational temperature of methanol was found to be  $16 \pm 7$  K,  $32 \pm 8$ , and  $25 \pm 4$  K on 7–8 September 1999, and

**Table 1.** Molecular observations in comet 10P/Tempel 2

	UT date [mm/dd.dd]	$\langle r_h \rangle$ [AU]	$\langle \Delta \rangle$ [AU]	Integ. time [min] <sup>a</sup>	Line	Intensity [K km s <sup>-1</sup> ]	Velocity shift <sup>b</sup> [ km s <sup>-1</sup> ]	Prod. rate [molec. s <sup>-1</sup> ]
1999 perihelion passage:								
JCMT	09/04.2–06.3	1.482	0.816	157	HCN(4–3)	0.058 ± 0.012	−0.86 ± 0.23	0.5 ± 0.1 × 10 <sup>25</sup>
CSO	09/11.2–12.3	1.482	0.851	133	HCN(3–2)	0.106 ± 0.012	−0.20 ± 0.08	1.4 ± 0.2 × 10 <sup>25</sup>
CSO	09/12.32	1.482	0.855	72	CH <sub>3</sub> OH(4 <sub>1</sub> – 4 <sub>0</sub> A-+)	0.080 ± 0.018	+0.19 ± 0.15	3.7 ± 1.0 × 10 <sup>26</sup>
					CH <sub>3</sub> OH(2 <sub>1</sub> – 2 <sub>0</sub> A-+)	0.119 ± 0.016	−0.10 ± 0.08	
JCMT	10/01.3–02.3	1.500	0.980	67	HCN(3–2)	0.090 ± 0.019	−0.57 ± 0.18	0.9 ± 0.2 × 10 <sup>25</sup>
2010 perihelion passage:								
IRAM	07/07.28	1.423	0.745	126	HCN(1–0)	0.057 ± 0.013	−0.16 ± 0.16	1.6 ± 0.4 × 10 <sup>25</sup>
IRAM	07/08.26	1.423	0.742	131	HCN(1–0)	0.054 ± 0.009	−0.44 ± 0.14	1.5 ± 0.2 × 10 <sup>25</sup>
IRAM	07/10.22	1.424	0.734	103	HCN(3–2)	0.410 ± 0.033	−0.30 ± 0.05	1.5 ± 0.1 × 10 <sup>25</sup>
IRAM	07/10.34	1.424	0.734	42	HCN(1–0)	0.044 ± 0.016	−0.65 ± 0.33	1.2 ± 0.4 × 10 <sup>25</sup>
IRAM	07/11.17	1.424	0.731	61	HCN(3–2)	0.427 ± 0.036	−0.41 ± 0.05	1.6 ± 0.2 × 10 <sup>25</sup>
IRAM	07/11.28	1.424	0.731	131	HCN(1–0)	0.068 ± 0.010	−0.49 ± 0.13	1.8 ± 0.3 × 10 <sup>25</sup>
IRAM	07/07.2-08.4	1.423	0.743	257	CH <sub>3</sub> OH(1 <sub>0</sub> – 1 <sub>-1</sub> E)	0.028 ± 0.010	−0.41 ± 0.10 <sup>c</sup>	3.2 ± 0.8 × 10 <sup>26</sup>
					CH <sub>3</sub> OH(2 <sub>0</sub> – 2 <sub>-1</sub> E)	0.044 ± 0.010		
					CH <sub>3</sub> OH(3 <sub>0</sub> – 3 <sub>-1</sub> E)	0.032 ± 0.010		
					CH <sub>3</sub> OH(4 <sub>0</sub> – 4 <sub>-1</sub> E)	0.050 ± 0.010		
					CH <sub>3</sub> OH(5 <sub>0</sub> – 5 <sub>-1</sub> E)	0.030 ± 0.010		
					CH <sub>3</sub> OH(6 <sub>0</sub> – 6 <sub>-1</sub> E)	0.036 ± 0.010		
					CH <sub>3</sub> OH(7 <sub>0</sub> – 7 <sub>-1</sub> E)	0.008 ± 0.010		
IRAM	07/11.26	1.424	0.731	98	CH <sub>3</sub> OH(1 <sub>0</sub> – 1 <sub>-1</sub> E)	0.024 ± 0.008	−0.42 ± 0.08 <sup>c</sup>	3.2 ± 0.4 × 10 <sup>26</sup>
					CH <sub>3</sub> OH(2 <sub>0</sub> – 2 <sub>-1</sub> E)	0.046 ± 0.008		
					CH <sub>3</sub> OH(3 <sub>0</sub> – 3 <sub>-1</sub> E)	0.050 ± 0.008		
					CH <sub>3</sub> OH(4 <sub>0</sub> – 4 <sub>-1</sub> E)	0.041 ± 0.008		
					CH <sub>3</sub> OH(5 <sub>0</sub> – 5 <sub>-1</sub> E)	0.030 ± 0.008		
					CH <sub>3</sub> OH(6 <sub>0</sub> – 6 <sub>-1</sub> E)	0.017 ± 0.008		
					CH <sub>3</sub> OH(7 <sub>0</sub> – 7 <sub>-1</sub> E)	0.011 ± 0.008		
IRAM	07/10.34	1.424	0.734	42	H <sub>2</sub> S(1 <sub>10</sub> – 1 <sub>01</sub> )	0.065 ± 0.021	−0.43 ± 0.26	7.1 ± 2.3 × 10 <sup>26</sup>
IRAM	07/11.34	1.424	0.730	33	CS(3–2)	0.049 ± 0.011	−0.02 ± 0.14	1.5 ± 0.3 × 10 <sup>25</sup>
IRAM	07/11.34	1.424	0.730	33	CH <sub>3</sub> CN(8 <sub>K</sub> -7 <sub>K</sub> ) $K=0,1,2^d$	< 0.062		< 0.8 × 10 <sup>25</sup>
HIFI	07/18.9–19.3	1.431	0.708	54	H <sub>2</sub> O(1 <sub>10</sub> -1 <sub>01</sub> )	5.509 ± 0.005	−0.062 ± 0.001	2.2 ± 0.1 × 10 <sup>28</sup>
HIFI	07/18.9–19.3	1.431	0.708	54	NH <sub>3</sub> (1 <sub>0</sub> -0 <sub>0</sub> )	0.072 ± 0.005	−0.43 ± 0.06 <sup>e</sup>	10.0 ± 0.7 × 10 <sup>25</sup>

Note: <sup>a</sup> Total integration time, ON+OFF, or ON in frequency switching mode (JCMT and HIFI);

<sup>b</sup> Reference line frequencies (excepted for NH<sub>3</sub> – see text<sup>e</sup>) were taken from CDMS (Müller et al. 2005);

<sup>c</sup> value based on the average of the 6 strongest lines;

<sup>d</sup> Sum of the three transitions  $J_K = 8_0-7_0$ ,  $8_1-7_1$ , and  $8_2-7_2$ ;

<sup>e</sup> Doppler shift measured with respect to the barycentric position of the hyperfine structure of the line at 572498.160 MHz.

11 July 2010 (Fig. 6), respectively. These values are compatible with a gas temperature  $T_{\text{rot}} = 25$  K, but a closer inspection of the relative intensities of the lines reveals that the night-side temperature ( $v > 0$  km s<sup>-1</sup>)  $T_{\text{rot}} = 21 \pm 5$  K is lower than in the day-side jet:  $T_{\text{rot}} = 31 \pm 4$  K. We will use  $T_{\text{rot}} = 30$  K in the sunward jet and  $T_{\text{rot}} = 20$  K elsewhere.

A good fit is obtained with 44% of the outgassing in a narrow jet (opening angle 37° or  $0.1 \times 4\pi$  steradian) with gas velocity of 0.9 km s<sup>-1</sup>, and the remaining 90% of the sky contain 56% of the outgassing at 0.5 km s<sup>-1</sup>, as illustrated in Fig. 7. The synthetic line shapes obtained with this modelling provide a reasonable fit to the observed lines (Figs. 2, 4 and 5). We used the same model to analyse the H<sub>2</sub>O 557 GHz line (Fig. 1) and determine the water production rate  $Q_{\text{H}_2\text{O}}$  at the time of the NH<sub>3</sub> observations. However, we assumed  $x_{ne} = 0.15$  in the excitation model. This value best explains the brightness distribution of the 557 GHz line observed on 19 July (Szutowicz et al. 2011, 2012 in preparation) and is consistent with values found in other comets (Biver et al. 2007; Hartogh et al. 2010). The model reproduces both the line intensity and the Doppler shift of the water line if we set  $Q_{\text{H}_2\text{O}}$  to

$2.2 \times 10^{28}$  molec. s<sup>-1</sup> (Table 1). This simplistic modelling of the anisotropic outgassing of comet 10P/Tempel 2 will be improved in a future paper (Szutowicz et al. 2012 in preparation), but is sufficient to derive accurate production rates and relative abundances. When isotropic outgassing is assumed and the gas temperature set to 25 K, we derive production rates  $\approx 15\%$  higher for the short-lived molecules like H<sub>2</sub>S and NH<sub>3</sub>, or  $\approx 45\%$  higher for other molecules.

### 3.2. Ammonia

The ammonia  $J_K$  (1<sub>0</sub>-0<sub>0</sub>) line at 572.5 GHz is clearly detected (Fig. 2). The hyperfine structure of the ammonia line is similar to that of the  $J$  (1–0) HCN line: three components  $F$  (2–1),  $F$  (1–1) and  $F$  (0–1) with relative intensities 5, 3 and 1, and relative velocities at 0.0, +0.64 and −0.97 km s<sup>-1</sup>, respectively, with respect to the  $F$  (2–1) frequency of 572498.371 MHz (Cazzoli et al. 2009). This structure is resolved in the observed spectrum of NH<sub>3</sub> (Fig. 2). The synthetic line profile, based on a model used to fit the optically thin molecular lines observed at

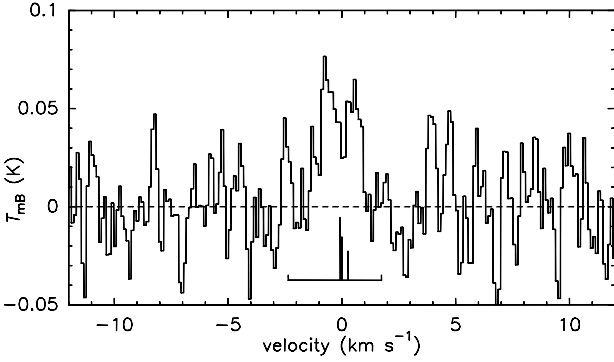


**Fig. 3.** HCN  $J(3-2)$  line at 265.886 GHz observed in comet 10P/Tempel 2 with the CSO on 11–12 September 1999. The positions and relative intensities of the hyperfine components are drawn as detailed in Fig. 4.

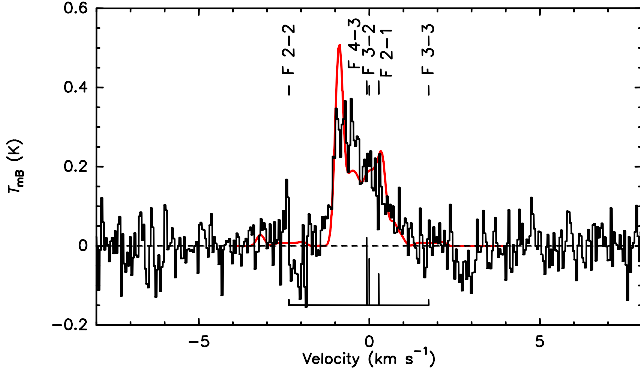


**Fig. 4.** HCN  $J(3-2)$  line at 265.886 GHz observed in comet 10P/Tempel 2 with the IRAM 30-m telescope on 10–11 July 2010. The position and relative intensities of the hyperfine components are shown and a synthetic spectrum including asymmetric outgassing (see text) and hyperfine structure is overplotted.

IRAM (Figs 4 and 5, Section 3.1), agrees well with the observed profile.

The time variation of the line intensity is marginal ( $\pm 17\%$ , at a  $1.5\text{-}\sigma$  level of significance). The ammonia production rate was derived with the previously described collision and outgassing pattern model. We assumed a total cross-section of  $2 \times 10^{-14} \text{ cm}^2$  for the collisions with neutrals. Collisions with electrons were modelled in the same way as for the other molecules (e.g. Zakharov et al. 2007), i.e. we used the Born approximation for the computation of the cross-sections and set  $x_{ne} = 0.5$ . Infrared pumping through the six strongest ( $\nu_1$ ,  $\nu_2$ ,  $\nu_3$ ,  $\nu_4$ ,  $\nu_3 + \nu_4$ , and  $\nu_2 + \nu_3$ ) vibrational bands was taken into account using the GEISA database (Jacquinet-Husson et al. 2008). Table 2 lists the pumping rates for the main infrared bands of ammonia. The six bands included in our model comprise 95% of the infrared pumping. Our excitation rates agree with those of Kawakita & Mumma (2011). When computing the fluorescence of the vibrational bands down to the fundamental ground state,

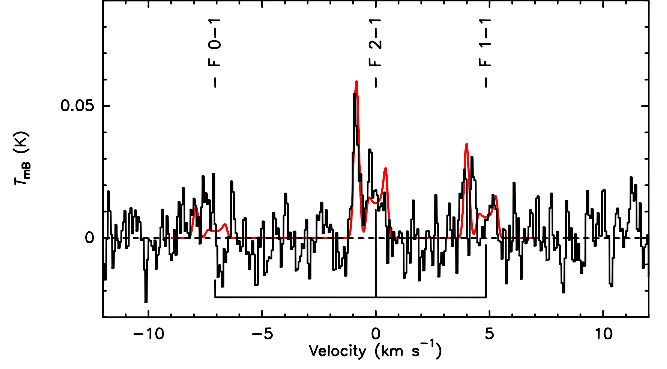


**Fig. 5.** HCN  $J(1-0)$  line at 88.632 GHz observed in comet 10P/Tempel 2 with the IRAM 30-m telescope on 7–11 July 2010. The position and relative intensities of the hyperfine components are shown and a synthetic spectrum considering asymmetric outgassing (see text) is overplotted.

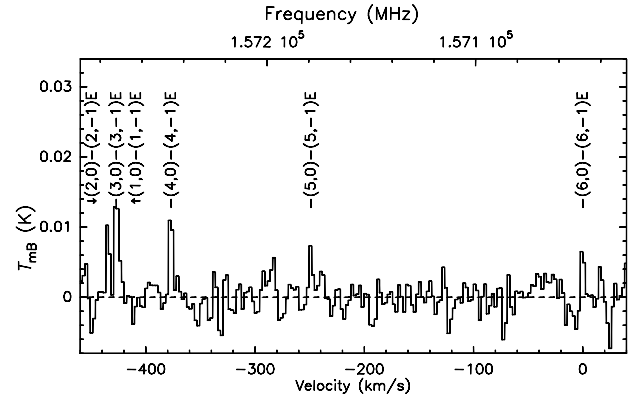


**Fig. 6.** CH<sub>3</sub>OH lines at 157 GHz observed in comet 10P/Tempel 2 with the IRAM 30-m telescope on 11 July 2010.

we did not consider that the  $\nu_3 + \nu_4$ , and  $\nu_2 + \nu_3$  bands partly deexcite via  $\nu_3$ . Since these combination bands are weak, this approximation should not affect significantly the rotational populations. The radial evolution of the population of the six lowest ortho levels of NH<sub>3</sub> is shown in Fig. 8.

The NH<sub>3</sub> photodissociation rate is  $\beta_0 = 1.8 \times 10^{-4} \text{ s}^{-1}$  for the quiet Sun at  $r_h = 1 \text{ AU}$  (Huebner et al. 1992). Because the NH<sub>3</sub> lifetime is relatively short, radiative processes do not significantly affect the excitation of the rotational levels for comets with high outgassing rates. Indeed NH<sub>3</sub> photodissociates before reaching the rarefied coma where IR pumping and radiative decay dominate over collisional excitation. For moderately active comets like 10P/Tempel 2, these processes are significant: neglecting IR pumping would overestimate the production rate by a factor 2.5 and assuming thermal equilibrium would underestimate it by a factor 1.7. On the other hand, neglecting the anisotropy of the outgassing would increase the production rate by only 14%. The derived ammonia production rate is  $1.0 \times 10^{26} \text{ molec. s}^{-1}$ . The contemporaneous water production being  $\approx 2.2 \times 10^{28} \text{ molec. s}^{-1}$  (Table 1), we obtain  $[\text{NH}_3]/[\text{H}_2\text{O}]$

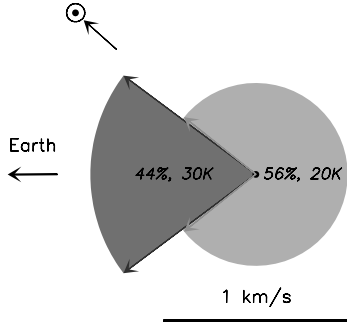


**Fig. 7.** Outgassing pattern used to interpret 10P/Tempel 2 observations. The length of the vectors pointing away from the nucleus are proportional to the expansion velocity (scale bar). The shaded area in dark represents the earthward jet at  $0.9 \text{ km s}^{-1}$  containing 44% of the outgassing with a  $T = 30 \text{ K}$  temperature, while the lightly shaded area represents the remaining part of the sky with lower velocity ( $0.5 \text{ km s}^{-1}$ ) and temperature ( $20 \text{ K}$ ).

**Table 2.** Ammonia infrared band parameters and excitation rates

vibrational band	frequency [ $\text{cm}^{-1}$ ]	$A_v^a$ [ $\text{s}^{-1}$ ]	$g_v^a$ at 1 AU [ $\text{s}^{-1}$ ]	used
$\nu_1$	3337	7.7	$3.3 \times 10^{-5}$	yes
$\nu_2$	$\approx 950$	16.2	$27.7 \times 10^{-5}$	yes
$2\nu_2$	$\approx 1700$	0.5	$0.5 \times 10^{-5}$	no
$3\nu_2$	$\approx 2600$	0.1	$0.05 \times 10^{-5}$	no
$\nu_1 + \nu_2$	4315	1.6	$0.5 \times 10^{-5}$	no
$\nu_3$	3450	3.8	$1.5 \times 10^{-5}$	yes
$\nu_4$	1630	8.7	$8.5 \times 10^{-5}$	yes
$\nu_2 + \nu_4$	2600	0.02	$0.01 \times 10^{-5}$	no
$\nu_3 + \nu_4$	5000	15	$3.7 \times 10^{-5}$	yes
$\nu_1 + \nu_4$	4960	0.6	$0.2 \times 10^{-5}$	no
$\nu_2 + \nu_3$	4450	9	$2.6 \times 10^{-5}$	yes
$2\nu_4$	3240	2.7	$0.4 \times 10^{-5}$	no

Note: <sup>a</sup> “Band” (as defined in Crovisier & Encrenaz 1983) Einstein coefficients and total excitation rates (from GEISA database (Jacquinet-Husson et al. 2008)) computed at  $40 \text{ K}$ .

$= 0.46 \pm 0.04\%$ . This value is very similar to the abundance measured in other comets (Kawakita & Watanabe 2002; Biver et al. 2007; Kawakita & Mumma 2011).

The ortho-to-para ratio (OPR) of ammonia is not directly measured in comets; it is inferred from that of the  $\text{NH}_2$  radical and found to be typically 1.1 to 1.2, corresponding to spin temperatures  $\approx 30 \text{ K}$  (Kawakita et al. 2001; Shinnaka et al. 2010, 2011). When analysing our measurement, where only *ortho*  $\text{NH}_3$  was observed, we assumed  $\text{OPR} = 1$  (statistical ratio). Therefore, our determination of the production rate may be overestimated by 5 to 10%.

### 3.3. Molecular abundances from ground based data

Table 1 provides production rates inferred for HCN and  $\text{CH}_3\text{OH}$  in 1999, and for HCN,  $\text{CH}_3\text{OH}$ , CS,  $\text{H}_2\text{S}$  and  $\text{CH}_3\text{CN}$  in 2010. Based on contemporaneous water production of  $\approx 1.8 \times 10^{28} \text{ molec. s}^{-1}$  (Szutowicz et al. 2012 in preparation) at the

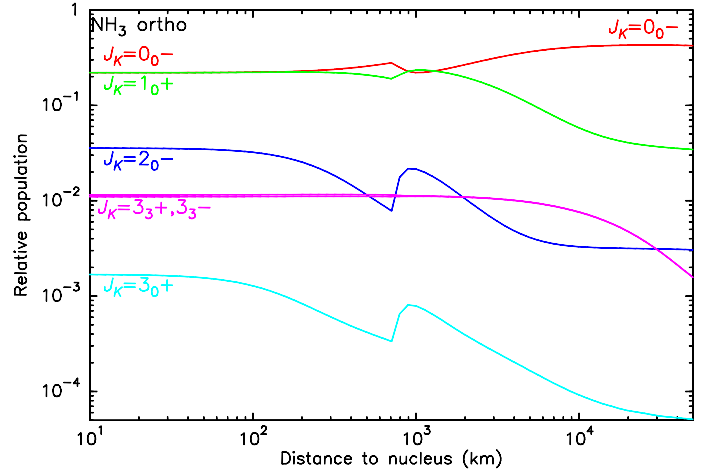


**Fig. 8.** Rotational populations of the lowest ortho levels of  $\text{NH}_3$  in the coma of comet 10P/Tempel 2 ( $r_h = 1.431 \text{ AU}$ ,  $Q_{\text{H}_2\text{O}} = 2.2 \times 10^{28} \text{ molec. s}^{-1}$ ,  $v_{\text{exp}} = 0.7 \text{ km s}^{-1}$ ), taking into account collisions with neutrals at  $T = 25 \text{ K}$ , collisions with electrons (responsible for the feature at the contact surface at  $\approx 1000 \text{ km}$ ), radiative decay and infrared pumping.

**Table 3.** Molecular abundances in comet 10P/Tempel 2

Molecule	$Q/Q_{\text{HCN}}$ in 1999	$Q/Q_{\text{HCN}}$ in 2010	$Q/Q_{\text{H}_2\text{O}}$ in 2010
HCN	1	1	$0.09 \pm 0.01\%$
$\text{CH}_3\text{OH}$	$20 \pm 5$	$21 \pm 3$	$1.8 \pm 0.2\%$
$\text{H}_2\text{S}$		$4.6 \pm 1.6$	$0.39 \pm 0.13\%$
CS		$0.9 \pm 0.2$	$0.08 \pm 0.02\%$
$\text{CH}_3\text{CN}$		$< 0.5$	$< 0.04\%$
$\text{NH}_3$		-	$0.46 \pm 0.04\%$

time of IRAM observations in 2010 (i.e.  $\approx 9$  days earlier than the  $\text{NH}_3$  observation), the derived molecular abundances are given in Table 3. These abundances are typical of short-period comets, with  $\text{CH}_3\text{OH}$  and  $\text{H}_2\text{S}$  abundances in the middle-low part of the observed range (Crovisier et al. 2009a,b). The average cometary  $[\text{CS}]/[\text{HCN}]$  ratio is close to 0.8 at  $r_h = 1 \text{ AU}$ , with a  $r_h^{-0.8}$  dependence (Biver et al. 2006, 2011). The observed value in 10P/Tempel 2 is on the high side given that we would expect a value around 0.6 at  $r_h = 1.42 \text{ AU}$ . Ammonia is the dominant source of nitrogen in the cometary ices ( $\approx 80\%$ ). Other possible sources of nitrogen in comets are HNC, and  $\text{HC}_3\text{N}$ , which were always below the HCN abundance in all comets in which they were detected or searched for (e.g., Bockelée-Morvan et al. 2004). Note that even though  $\text{HC}_3\text{N}$  was not searched in depth in comet 10P, low-resolution spectra on 11.3 July provide an upper limit on the  $\text{HC}_3\text{N } J(16-15)$  line, which yields in any case  $Q_{\text{HC}_3\text{N}} < 0.3 \times Q_{\text{NH}_3}$ .

In 1999 the comet had a higher activity on 12 September when  $\text{CH}_3\text{OH}$  was observed and HCN reached a maximum. At other dates, however, it was at least 50% less active than in 2010. This is likely due to a larger perihelion distance (1.48 vs 1.42 AU). Meanwhile, the  $[\text{CH}_3\text{OH}]/[\text{HCN}]$  ratio did not change in 11 years after two orbits around the Sun and the prominent jet feature was still there: the line asymmetry is still present and visible images showed a similar northwards jet structure (Biver personal communication) at both apparitions.

## 4. Conclusion

Ammonia was directly observed in comet 10/Tempel 2 through its fundamental rotational line. The hyperfine structure of the line is resolved for the first time in an astronomical object, thanks to the narrow width of the cometary line. The abundance of ammonia is found to be  $0.46 \pm 0.04\%$  relative to water. This is similar to values measured in other comets, making ammonia the major source of nitrogen in cometary ices. The abundances of HCN, CH<sub>3</sub>OH, CS, and H<sub>2</sub>S are typical of short-period comets, though on the mid-low range. The comet displayed strongly blueshifted lines indicative of a strong asymmetry in the outgassing. This asymmetry is present for all species, which also suggests a common source for all and compositional homogeneity. Based on simple modelling, about half of the outgassing is in a narrow sunward jet with a higher outgassing speed ( $0.9 \text{ km s}^{-1}$ ) than outside the jet ( $0.5 \text{ km s}^{-1}$ ).

*Acknowledgements.* HIFI has been designed and built by a consortium of institutes and university departments from across Europe, Canada and the United States under the leadership of SRON Netherlands Institute for Space Research, Groningen, The Netherlands and with major contributions from Germany, France and the US. Consortium members are: Canada: CSA, U. Waterloo; France: CESR, LAB, LERMA, IRAM; Germany: KOSMA, MPIfR, MPS; Ireland: NUI Maynooth; Italy: ASI, IFSI-INAF, Osservatorio Astrofisico di Arcetri-INAF; Netherlands: SRON, TUD; Poland: CAMK, CBK; Spain: Observatorio Astronómico Nacional (IGN), Centro de Astrobiología (CSIC-INTA); Sweden: Chalmers University of Technology – MC2, RSS & GARD; Onsala Space Observatory; Swedish National Space Board, Stockholm University – Stockholm Observatory; Switzerland: ETH Zurich, FHNW; USA: Caltech, JPL, NHSC. We are grateful to the IRAM staff and to other observers for their assistance during the observations. IRAM is an international institute co-funded by the Centre national de la recherche scientifique (CNRS), the Max Planck Gesellschaft and the Instituto Geográfico Nacional, Spain. This research has been supported by the CNRS and the Programme national de planétologie de l'Institut des sciences de l'univers (INSU). The CSO is supported by National Science Foundation grant AST-0540882. The James Clerk Maxwell Telescope is operated by The Joint Astronomy Centre on behalf of the Science and Technology Facilities Council of the United Kingdom, the Netherlands Organisation for Scientific Research, and the National Research Council of Canada. The research leading to these results received funding from the European Community's Seventh Framework Programme (FP7/2007–2013) under grant agreement No. 229517. S.S. was supported by MNIW (grant 181/N-HSO/2008/0).

## References

- Altenhoff, W. J., Batrla, W. K., Huchtmeier, W. K., et al. 1983, *A&A*, 125, L19  
 Bird, M. K., Huchtmeier, W. K., von Kap-Herr, A., Schmidt, J. & Walmsley, C. M. 1987, in *Cometary Radio Astronomy*, ed W. M. Irvine, F. P. Schloerb, & L. E. Tacconi-Garman, (Green Bank, WV, National Radio Astronomy Observatory), 85  
 Bird, M. K., Huchtmeier, W. K., Gensheimer, P., et al. 1997, *A&A*, 325, L5  
 Bird, M. K., Hatchell, J., van der Tak, F. F. S., Crovisier, J. & Bockelée-Morvan, D. 2002, In *Proceedings of Asteroids, Comets, Meteors - ACM 2002*, ed. Barbara Warmbein, ESA SP-500, 697  
 Biver, N., Bockelée-Morvan, D., Crovisier, J., et al. 2006, *A&A*, 449, 1255  
 Biver, N., Bockelée-Morvan, D., Crovisier, J., et al. 2007, *Planet. Space Sci.*, 55, 1058  
 Biver, N., Szutowicz, S., Bockelée-Morvan, D., et al. 2010, *BAAS*, 42, 946  
 Biver, N., Bockelée-Morvan, D., Colom, P., et al. 2011, *A&A*, A142  
 Bockelée-Morvan, D., Crovisier, J., Mumma, M. J., & Weaver, H. A. 2004, in *Comets II*, ed. M. C. Festou, H. U. Keller, & H. A. Weaver (Univ. of Arizona Press), 391  
 Cazzoli, G., Dore, L., & Pizzarini, C. 2009, *A&A*, 507, 1707  
 Crovisier, J., & Encrenaz, Th. 1983, *A&A*, 126, 170  
 Crovisier, J., Biver, N., Bockelée-Morvan, D., & Colom, P. 2009a, *Planet. Space Sci.*, 57, 1162  
 Crovisier, J., Biver, N., Bockelée-Morvan, D., et al. 2009b, *Earth Moon and Planets*, 105, 267  
 de Graauw, T., Helmich, F. P., Phillips, T. G., et al. 2010, *A&A*, 518, L6  
 Feldman, P. D., Cochran, A. L., & Combi, M. R. 2004, in *Comets II*, ed. M. C. Festou, H. U. Keller, & H. A. Weaver (Univ. of Arizona Press), 425

- Jacquinet-Husson, N., Scott, N. A., Chédin, A., et al. 2008, *J. Quant. Spec. Radiat. Transf.*, 109, 1043  
 Hartogh, P., Lellouch, E., Crovisier, J., et al. 2009, *Planet. Space Sci.*, 57, 1596  
 Hartogh, P., Crovisier, J., de Val-Boro, M., et al. 2010, *A&A*, 518, L150  
 Hatchell, J., Bird, M. K., van der Tak, F. F. S., & Sherwood, W. A., 2005, *A&A*, 439, 777  
 Hirota, T., Yamamoto, S., Kawaguchi, K., Sakamoto, A., & Ukita, N. 1999, *A&A*, 520, 895  
 Huebner, W. F., Keady, J. J., & Lyon, S. P. 1992, *Ap&SS*, 195, 1  
 Jewitt, D., & Luu, J. 1989, *AJ*, 97, 1766  
 Kawakita, H., Watanabe, J.-i., Ando, H., et al. 2001, *Science*, 294, 1089  
 Kawakita, H., & Mumma, M. J. 2011, *ApJ*, 727, 91  
 Kawakita, H., & Watanabe, J.-i. 2002, *ApJ*, 572, L177  
 Knight, M. M., Farnham, T. L., Schleicher, D. G., Schwieterman, E. W. 2011, *AJ*, 141, 2  
 Lamy, P. L., Toth, I., Weaver, H. A., A'Hearn, M. F., & Jorda, L. 2009, *A&A*, 508, 1045  
 Müller, H. S. P., Schlöder, F., Stutzki J. & Winnewisser, G. 2005, *J. Mol. Struct.* 742, 215 (<http://www.astro.uni-koeln.de/cdms/>)  
 Palmer, P., Wootten, A., Butler, B., et al. 1996, *BAAS*, 28, 927  
 Pilbratt, G. L., Riedinger, J. R., Passvogel, T., et al. 2010, *A&A*, 518, L1  
 Shinnaka, Y., Kawakita, H., Kobayashi, H., & Kanda, Y.-I. 2010, *PASJ*, 62, 263  
 Shinnaka, Y., Kawakita, H., Kobayashi, H., et al. 2011, *ApJ*, 729, 81  
 Szutowicz, S., Biver, N., Bockelée-Morvan, D., et al. EPSC-DPS Joint Meeting, 2-7 October 2011, Nantes, France 2011, EPSC Abstracts Vol. 6, EPSC-DPS2011-1213  
 Szutowicz, S., et al., in preparation  
 Zakharov, V., Bockelée-Morvan, D., Biver, N., Crovisier, J., & Lecacheux, A. 2007, *A&A*, 473, 303